



HAL
open science

Interactions between smectites and polyelectrolytes

Cheng Cheng Shen, Sabine Petit, Cun Jun Li, Chun Sheng Li, Nafeesa Khatoon, Chun Hui Zhou

► **To cite this version:**

Cheng Cheng Shen, Sabine Petit, Cun Jun Li, Chun Sheng Li, Nafeesa Khatoon, et al.. Interactions between smectites and polyelectrolytes. *Applied Clay Science*, 2020, 198, pp.105778. 10.1016/j.clay.2020.105778 . hal-03000670

HAL Id: hal-03000670

<https://hal.science/hal-03000670>

Submitted on 2 Dec 2020

HAL is a multi-disciplinary open access archive for the deposit and dissemination of scientific research documents, whether they are published or not. The documents may come from teaching and research institutions in France or abroad, or from public or private research centers.

L'archive ouverte pluridisciplinaire **HAL**, est destinée au dépôt et à la diffusion de documents scientifiques de niveau recherche, publiés ou non, émanant des établissements d'enseignement et de recherche français ou étrangers, des laboratoires publics ou privés.

Interactions between Smectites and Polyelectrolytes

Cheng Cheng Shen^{a,c}, Sabine Petit^d, Cun Jun Li^a, Chun Sheng Li^b, Nafeesa Khatoona, Chun Hui Zhou^{a,b,c,□}

^a Research Group for Advanced Materials & Sustainable Catalysis (AMSC), State Key Laboratory Breeding Base of Green Chemistry-Synthesis Technology, College of Chemical Engineering, Zhejiang University of Technology, Hangzhou 310032, China

^b Key Laboratory of Clay Minerals of Ministry of Land and Resources of the People's Republic of China, Engineering Research Center of Non-metallic Minerals of Zhejiang Province, Zhejiang Institute of Geology and Mineral Resource, Hangzhou 310007, China

^c Qing Yang Institute for Industrial Minerals, You Hua, Qing Yang, Chi Zhou 242804, China

^d Institut de Chimie des Milieux et Matériaux de Poitiers (IC2MP), UMR 7285 CNRS, Université de Poitiers, Poitiers Cedex 9, France

Corresponding author: Prof. Chun Hui ZHOU. E-mail: clay@zjut.edu.cn

Abstract

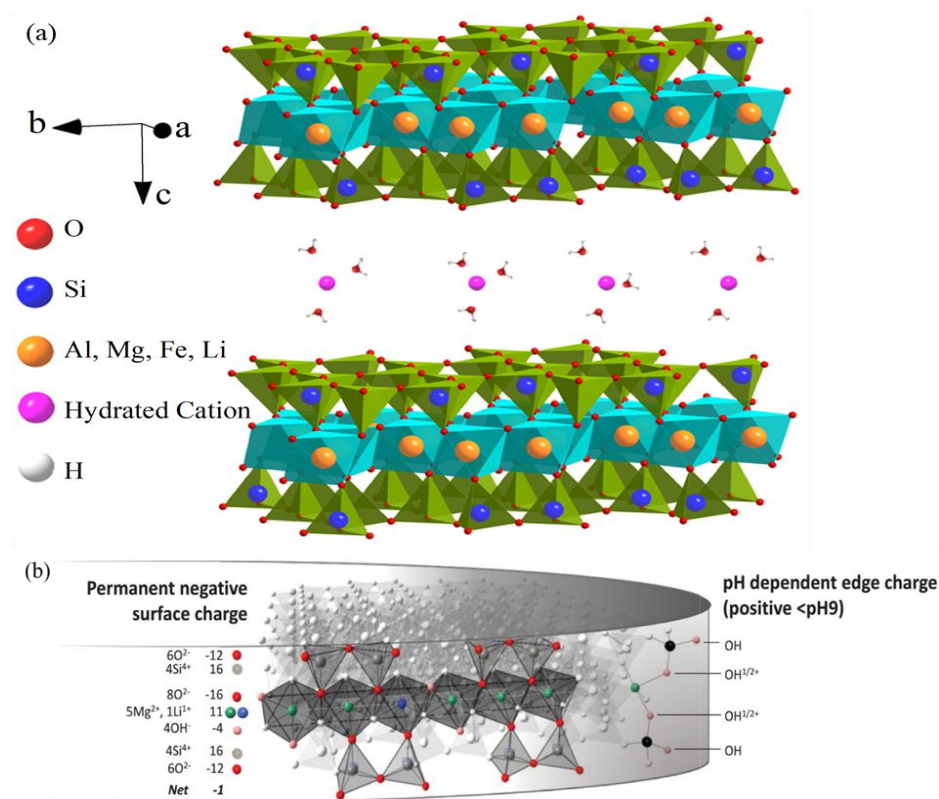
Interactions between smectite and polyelectrolyte play an essential role in exclusive adsorption, flocculation, and thixotropic properties of aqueous smectite/polyelectrolyte system. The materials are widely used in many industries such as drilling fluids, pharmaceuticals, paints and dyes, ceramics, papermaking and water treatment. This review focuses on the interaction between different types of polyelectrolytes and smectite, and their applications in flocculation and industrial wastewaters. The effect of several parameters related to polyelectrolyte such as charge density, charge type and molecular weight, as well as to smectite such as type, particle size, composition, pH and concentration in the aqueous system, were examined. The interactive forces between smectite and polyelectrolyte including hydrophobic interaction, ion binding, hydrogen bonding, van der Waals forces and electrostatic were thoroughly discussed. The interactive forces between smectite and cationic polyelectrolyte, anionic polyelectrolyte and amphoteric polyelectrolyte influence the flocculation of colloidal smectite-polyelectrolyte dispersions such as settling and floc dispersion. However, the interaction between smectites and polyelectrolytes and their subsequent behaviors in adsorption, flocculation, and thixotropy along with inherent mechanisms have not yet fully understood. Future in-depth work on interactions between smectites and polyelectrolytes has great implications for developing functional materials and expanding applications of other polyelectrolyte/ smectite mineral system.

Keywords: Smectites; Polyelectrolytes; Interaction; Adsorption; Flocculation; Rheology.

38
39
40
41
42
43
44
45
46
47
48
49
50
51
52
53
54

1. Introduction

Smectite refers to a family of layered aluminosilicate that possesses peculiar cation exchange capacity (CEC), surface reactivity and adsorption. Typically, smectite's layered structure is composed of -Si-O-Mg (Al or Li)-O-Si- layers separated by hydrated cations (e.g. Na⁺, NH₄⁺, Li⁺, K⁺ and Mg²⁺) in the interlayer space where each layer consists of two Si-O-Si tetrahedral sheets sandwiching an octahedral sheet (**Fig. 1a**). According to how much the center space of the octahedron is occupied with metal cation, clay minerals in smectite family are divided into dioctahedral ones such as montmorillonite, and trioctahedral one such as saponite and hectorite (Bergaya and Lagaly, 2013; Ismadji et al., 2015). A commercially available synthetic hectorite is known as laponite[®]. Montmorillonite, saponite and hectorite have physical and chemical properties in swelling and delamination. The layers have amphoteric properties and carry a permanent negative charge and localized positive charges (or negative charges at high pH, pH>9) (Sposito et al., 1999; Dawson and Oreffo, 2013) (**Fig. 1b**). The layers and relevant smectite particles readily give rise to interactions between the smectite particle surfaces and polyelectrolytes including hydrogen bonding, hydrophobic interactions, ion binding, van der Waals forces, electrostatic attraction, and electrostatic repulsion (Song et al., 2010).



55
56
57
58
59
60

Fig.1. Smectite and its surface properties (a) The structure of smectite: layer is composed of two tetrahedral silica sheets sandwiching an octahedral sheet (with Al³⁺, Li⁺, Mg²⁺, and Fe²⁺ or Fe³⁺ as octahedral cations). Charge deficiencies in the octahedral and/or tetrahedral sheets yield a negative surface charge balanced by exchangeable cations in the interlayer space. (b) Smectites possess a permanent negative surface charge arising from isomorphous substitutions in the crystal structure and a pH dependent edge charge from unsatisfied valences in the disrupted

61 crystal lattice. Reprinted from. (Reprinted by permission from John Wiley and Sons: (Dawson and Oreffo, 2013),
62 copyright 2013).

63

64 Smectites and polyelectrolytes are widely used in pharmaceuticals, drilling fluids, water
65 treatment, ceramics, papermaking, paints and dyes (Carli et al., 2015; Xiao et al., 2016).
66 Polyelectrolytes are a class of specific polymers of which repeating units bear electrolyte groups.
67 They can be categorized into cationic, anionic and amphoteric polyelectrolytes. These
68 polyelectrolytes can coexist with smectite in water and can vary their properties such as the
69 adsorption, flocculation rheology and thixotropy primarily due to interaction between aqueous
70 smectite and polyelectrolytes (Kim and Carty, 2016; Shaikh et al., 2017a). Hence, the interaction
71 between smectite and polyelectrolyte has captured many researchers' interest and attention. The
72 relevant applications and implications have been significantly widened (**Fig. 2b**).

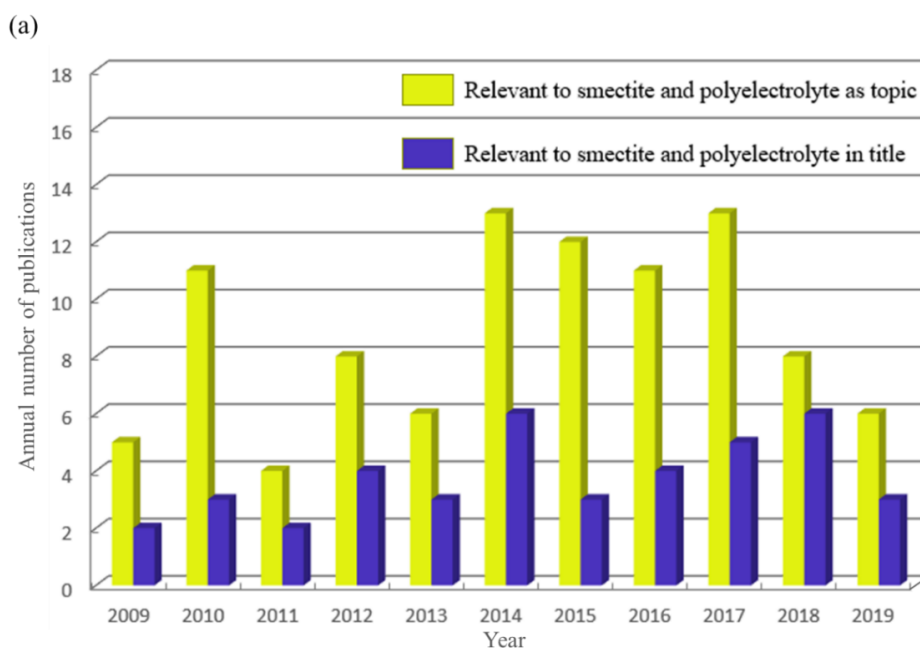
73 The interactions between smectite and polyelectrolyte depend on the physical and chemical
74 properties of smectites, polyelectrolytes, and medium. The polymeric structure of the
75 polyelectrolyte, the chemical structure of monomer in the backbone, the charge distribution in
76 monomeric groups and their distribution along the polyelectrolyte chains, are influential (Shaikh
77 et al., 2017b). The polyelectrolyte concentration in water, molecular weight and functional groups
78 are also critically important for the interactions between smectite and polyelectrolyte. In addition,
79 the smectite–polyelectrolyte interactions in aqueous medium also depend on the size, shape,
80 surface charge, and concentration of the smectite particles. Besides the pH and the temperature,
81 the medium also has an impact on the smectite–polyelectrolyte interactions in water (Alemdar et
82 al., 2005; Oliyaei et al., 2015).

83 Addition of polyelectrolytes into aqueous smectite dispersion remarkably modifies the
84 surface properties of the smectite and consequently changes the smectite particle–particle
85 interactions. This might lead to exclusive adsorptive (Abdullah et al., 2013), flocculent (Mansri et
86 al., 2019), rheological and thixotropic properties (Abu-Jdayil, 2011; Aalaie, 2012; Aydin et al.,
87 2015). These interactions between smectites and polyelectrolytes can be utilized in
88 pharmaceuticals (Viseras et al., 2010), oil and gas drilling fluids (Falode et al., 2008; Karagüzel
89 et al., 2010; Vipulanandan and Mohammed, 2014), paints and dyes (Wang et al., 2014),
90 paper-making industry (Zhang et al., 2013b), environmental remediation (Ismadji et al., 2015) and
91 water treatment of smectites (Lee et al., 2014; Santhosh et al., 2016). For example, smectites as
92 adsorbents and polyelectrolytes as flocculants are used for separation to treat industrial
93 wastewaters (Marchuk et al., 2016) due to their cost- effectiveness (Sievers et al., 2015),
94 versatility (Silva et al., 2016), high efficiency (Vereb et al., 2017) and relatively low toxicity (Van
95 Haver and Nayar, 2017). In drilling fluid, smectite nanoparticles, along with polyelectrolytes, has
96 been widely used to improve the rheology and filtration properties (Yu et al., 2018; Zhou et al.,
97 2016).

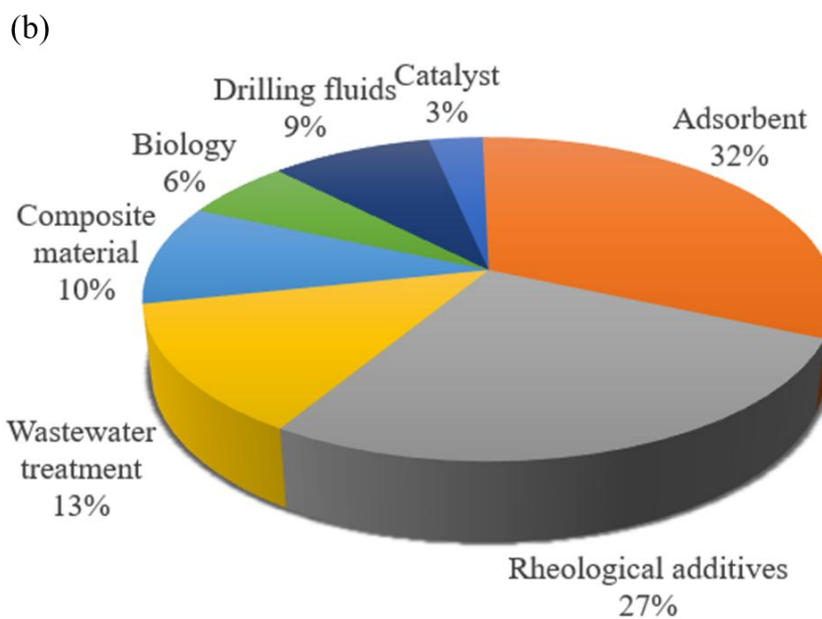
98 It is evident that interactions between smectites and polyelectrolytes are of great scientific
99 and technological significance (**Fig. 2a**). The study of such interactions has become greatly

100 multidisciplinary involving colloid and interface science, rheology, materials science, mineralogy
 101 and chemistry. Current research primarily focuses on the interaction between smectites and
 102 polyelectrolytes. Studies clearly reveal that the adsorption of polyelectrolytes to smectites affects
 103 their structure and chemical properties, flocculation and rheological behavior. Traditionally, the
 104 interaction between smectites and polyelectrolytes is used for developing adsorbent, flocculants,
 105 rheological additives and catalysts (**Fig. 2b**). Recently, this interaction is increasingly used for
 106 making hierarchical materials, tissue engineering materials, biosensors and drug carriers. For
 107 example, halloysite-polyelectrolytes interactions and illite-polyelectrolytes interactions has been
 108 intensively used for making biomedical composites (Zhao et al., 2015; Zhen et al., 2016; Tarasova
 109 et al., 2019).

110



111



112

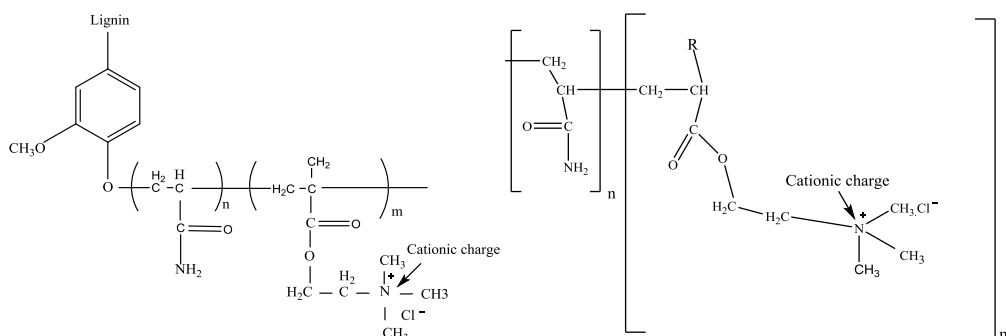
113 Fig. 2. (a) Annual number of peer-reviewed papers (published from 2009 to 2019) relevant to the topic of
114 interactions between polyelectrolytes and smectites. Data from Web of Science Core Collection and by searching
115 for terms in topic: smectites, polyelectrolytes and interactions; (b) Data from Web of Science Core Collection and
116 by searching for terms in topic: montmorillonite, polyelectrolytes and application, saponite, polyelectrolytes and
117 application, hectorite or laponite, polyelectrolytes and application, and Results Analysis according to
118 peer-reviewed scientific papers indexed in Web of Science Core Collection (published from 2009 to 2019).

119
120 In the present paper, the interactions between smectites (montmorillonite, saponite, and
121 hectorite) and polyelectrolytes (cationic, anionic, and amphoteric) are overviewed. The insights
122 into the effects of the interactions on adsorption, flocculation, and rheology and related
123 applications are critically examined. Then, the existing problems and challenges are analyzed and
124 discussed.

125 126 **2. Cationic polyelectrolytes**

127 **2.1 Montmorillonite**

128 Montmorillonite layer possesses negative charges while the layer edges have variable charges
129 at different pH whereas cationic polyelectrolytes bear positively charged functional groups. Kraft
130 lignin-acrylamide (KAD), polyacrylamide (PAM), tertiary amine methacrylate (TAM),
131 poly(acrylamide-co-(N-octyl-4-vinylpyridinium bromide)) and chitosan are typical cationic
132 polyelectrolytes which can readily interact with smectite (**Fig. 3**). The interactions subsequently
133 influence the adsorption, flocculation and rheological behavior of montmorillonite in water (**Table**
134 **1**). Generally, cationic polyelectrolytes induce flocculation via charge neutralization, patching,
135 polymer bridging, or combination of these interactions (Petzold and Schwarz, 2013, Zhou et al.,
136 2019a). Charged polyelectrolytes adsorbed on the surface of micro or nano form of
137 montmorillonite mainly through electrostatic interactions (Shaikh et al., 2017a). The amount of
138 adsorption mainly depends on the surface charge density of montmorillonite and the type of
139 charge of polyelectrolyte (Sakhawoth et al., 2017). Montmorillonite-polyelectrolyte system is
140 mostly used in agriculture (Ismadji et al., 2015), construction, drilling fluid (de Figueiredo et al.,
141 2014), and paints (de Figueiredo et al., 2014). It is also known to use in other fields such as
142 pharmaceuticals (Viseras et al., 2010), environmental remediation (Ismadji et al., 2015) and water
143 treatment (Beisebekov et al., 2014, Lee et al., 2014).

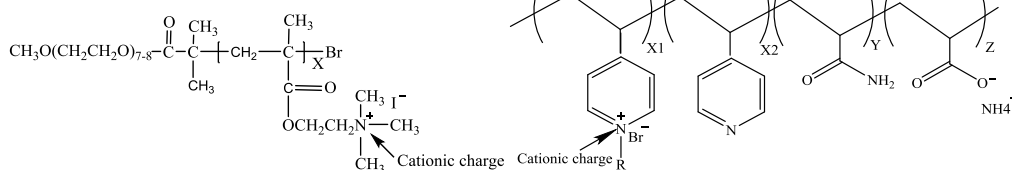


145

146

(a) Kraft lignin-acrylamide (Hasan and Fatehi, 2018)

(b) polyacrylamide (Craciun et al., 2015)

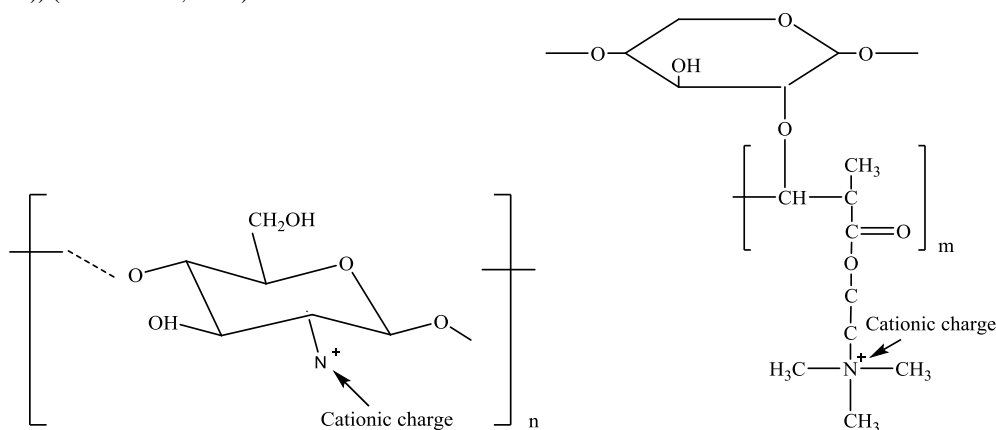


147

148

149

(c) Tertiary Amine Methacrylate (Alemdar and Bütün, 2005) (d) poly(acrylamide-co-(N-octyl-4-vinylpyridinium bromide)) (Mansri et al., 2019)



150

151

(e) Chitosan (Postnova et al., 2015)

(f) xylan-METAC (Wang et al., 2016)

152

153

154

Fig. 3. Chemical structures of the cationic polyelectrolytes used in recent studies relevant to the interaction between smectites and non-ionic polyelectrolytes

155

156

157

158

159

160

161

162

163

164

165

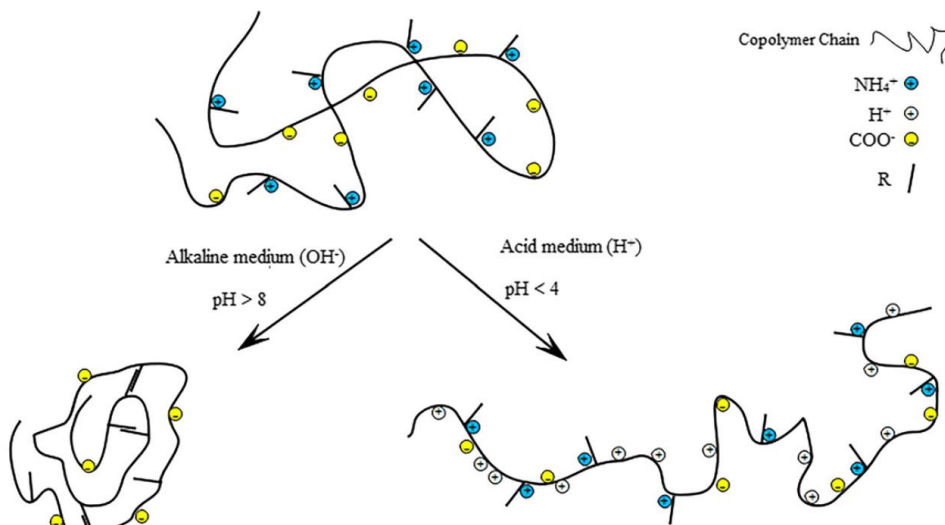
166

The surface charge density of montmorillonite and the molecular weight of cationic polyelectrolytes influence the adsorption and flocculation behavior of aqueous montmorillonite dispersion (Shaikh et al., 2017b). The floc sizes increased with increasing surface charge density and molecular weight of cationic polyelectrolytes. For example, interactions between the two kinds of cationic kraft lignin-acrylamide (KAD), of molecular weight 168,200 g/mol (KAD-1) and 103,000 g/mol (KAD-2) with montmorillonite has proved to be interact differently (Hasan and Fatehi, 2018). Although the two KADs had similar charge density (1.15 mmol/g), KAD-1, with a higher molecular weight, resulted in higher adsorption and bigger floc sizes than KAD-2. The KAD-1 and KAD-2 reached the saturation adsorption levels of 1.08 and 0.99 mg/g on montmorillonite, respectively. The KAD-1 would have a longer chain, therefore higher chance for tail and loop configuration on montmorillonite particles during adsorption of particles from the dispersion, which would in turn promote KAD-1 bridging. In addition, higher the charge density

167 of cationic KAD, greater is the adsorption and flocculation. For instance, an increase in the charge
168 density of a cationic KAD (KAD-1=2.13 meq/g, KAD-2=1.29 meq/g) promoted its adsorption
169 onto montmorillonite due to stronger electrostatic interactions between KAD and montmorillonite
170 particles. In case of montmorillonite, the adsorption for KAD-1 and KAD-2 was 1.83 and 1.63
171 mg/g, respectively. Similar phenomenon have been observed in the interactions for other
172 polyelectrolytes interacting with montmorillonite in water. (Wang et al., 2016) The flocculation
173 efficiency of cationic xylan-2-(methacryloyloxy)ethyl] trimethyl ammonium chloride
174 (xylan-METAC) copolymers with different charge density and different molecular weights were
175 compared where CMX1 and CMX2 has +1.8 and +2.4 meq/g with their molecular weights 88986
176 and 102545 g mol⁻¹, respectively. CMX2 was acted as a more efficient flocculant than CMX1 as
177 CMX2 adsorbed and removed more efficiently by montmorillonite particles from the aqueous
178 dispersion. The adsorption of CMX1 and CMX2 was 0.73 and 0.85 mg/g on montmorillonite
179 particles, respectively. It was reported that polymers with a higher charge density would adsorb
180 more on clay particles. CMX2 also changed the zeta potential and turbidity of the aqueous
181 montmorillonite dispersion more remarkably than CMX1, which was attributed to its higher
182 charge density and molecular weight.

183 In addition, different polyelectrolytes have different interactions with montmorillonite in
184 water. Polyelectrolytes such as 3,6-ionene (Campos and Tcacenco, 2015) interaction with the
185 montmorillonite surface takes place by Coulombic forces between the positively charged sites of
186 3,6- and negatively charged montmorillonite surface. The 3,6-ionene caused the basal spacing of
187 the commercial montmorillonite to increase from 1.5 to 3.5 nm. Polyelectrolytes such as
188 polycationic quaternary amine polymer F25 (Blachier et al., 2009), polyethyleneimine (PEI)
189 (Oztekin, 2017) and poly(acrylamide-co-(N-octyl-4-vinylpyridinium bromide)) (AM5/VP5C8Br)
190 were used to flocculate aqueous montmorillonite dispersion. The interactions between
191 AM5/VP5C8Br and montmorillonite particles in dilute aqueous dispersions (Mansri et al., 2019)
192 allowed the adsorption of the montmorillonite particles on the AM5/VP5C8Br chains, that
193 occurred initially by the hydrophobic interaction. The electrostatic attraction between the
194 positively charged sites on the AM5/VP5C8Br and the negative montmorillonite particles
195 dispersion can eventually lead to patches and flocculation. The AM5/VP5C8Br chain
196 conformation was affected by the pH of medium, thereby influencing the flocculation. The
197 AM5/VP5C8Br chains adopted a flat conformation at pH < 4 due to important repulsive
198 electrostatic forces by the cationic 4VP moieties (**Fig.4**). In the range of 4 < pH < 8, the charge
199 density of the AM5/VP5C8Br related to acid addition is very low, preventing the extension of the
200 AM5/VP5C8Br chains. At pH > 8, a turbidity removal becomes smaller than for pH < 4 and 4 <
201 pH < 8, which was related to the compact pelote conformation adopted by the AM5/VP5C8Br
202 chains. The hydroxide groups (OH) of aqueous medium played an important role in screening
203 phenomena of positively charged sites on the AM5/VP5C8Br chains. Thus, the flat conformation

204 assists the formation of flocs by adsorption between AM5/VP5C8Br and montmorillonite particles,
205 where the best flocculation was observed for dilute aqueous dispersions at pH <4.
206

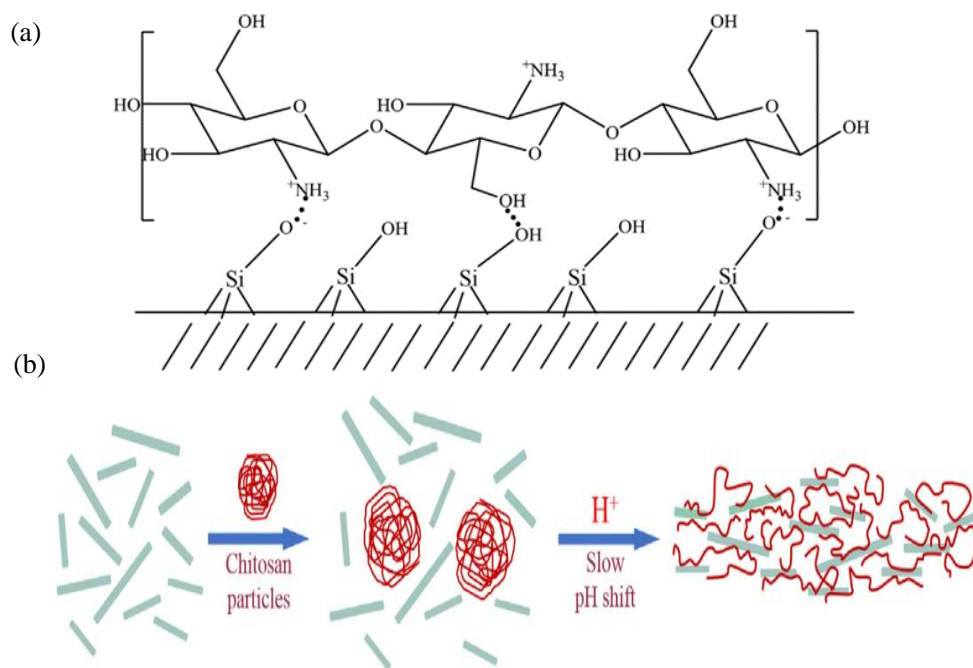


207
208 Fig.4 Proposed conformation of the AM5/VP5C8Br chain at different pH in aqueous medium. (Reprinted by
209 permission from Taylor & Francis: (Mansri et al., 2019), copyright 2019).
210

211 2.2 Saponite

212 Chitosan, a natural linear cationic polysaccharide containing free amino groups, has been
213 intercalated into saponite (Shchipunov et al., 2012a; Shchipunov et al., 2012b; Budnyak et al.,
214 2016; Mishchenko et al., 2016). Budnyak et al. (2016) demonstrated an effective way to produce
215 chitosan-saponite composites by impregnating 20g of saponite in 285ml of chitosan solution, with
216 a concentration of 7 mg/ml in acetic acid (pH 2.6). Chitosan has higher affinity for the surface of
217 saponite due to the interaction between protonated amino groups of chitosan and dissociated
218 saponite hydroxyl groups in water. The interactions also involve the electrostatic interaction and
219 hydrogen binding (**Fig. 5a**). The interaction between saponite and chitosan gradually increased the
220 viscosity and finally hydrogelation, leading to forming saponite/chitosan hydrogel nanocomposites
221 (**Fig. 5b**) (Zhou et al., 2019b). Budnyak et al. (2016) studied the adsorption properties of
222 chitosan-saponite composites for metal ions such as Cu(II), Zn(II), Fe(III), Cd(II), and Pb(II). The
223 results shows that the interactions between saponite and cationic chitosan improved the adsorption
224 of cations Cu(II), Zn(II), Fe(III), Cd(II), and Pb(II) due to excellent sorption properties of
225 chitosan-saponite composites and available adsorption sites in the interlayer space, large surface
226 area with narrower channels inside. Therefore, chitosan-saponite composites were employed to
227 adsorb the heavy metals and toxic dyes in wastewater treatment.

228



229

230 Fig. 5. (a) Schematic diagram showing that the interactions between chitosan and saponite involve the
 231 electrostatic interaction and hydrogen bonding (Budnyak et al., 2016); (b) Schematic drawing of main stages of
 232 formation of monolithic hydrogel by chitosan and saponite. (Shchipunov et al., 2009) – Reproduced by permission
 233 of The Royal Society of Chemistry.
 234

235

Table 1

236

Recent typical studies on the interaction between smectites and cationic polyelectrolytes

Cationic polyelectrolytes	Smectite	Conditions	Interaction	References
PAM	Montmorillonite	PAM: 2.0% v/v; Montmorillonite: 100 ml; The system: pH 9.	Strong adsorption affinity; Cause montmorillonite surface charge reversal; Floc sizes increased.	(Shaikh et al., 2017b)
AM5/VP5C8Br	Montmorillonite	AM5/VP5C8Br: 1–5 ppm; Montmorillonite: 400 ml; The system: pH 2.	Flocculation; Hydrophobic.	(Mansri et al., 2019)
xylan–METAC	Montmorillonite	Xylan–METACL: 2 or 3 mol mol ⁻¹ ; Montmorillonite concentration: 1 g L ⁻¹ ; pH 7.	Zeta potential and turbidity were changed; Higher charge density and molecular weight.	(Wang et al., 2016)
Chitosan	Saponite	Chitosan content: 285 ml; Saponite content: 20 g; Acetic acid concentration: 7 mg/ml; pH 2.6.	Electrostatic; Hydrogen binding.	(Budnyak et al., 2016)
RhPEG	Saponite	RhPEG content: 0.05–0.25wt%; Saponite 0.1 g L ⁻¹ ;	Irreversible adsorption; Two types of bonding between the	(Sas et al., 2017)

Poly(NIPAm)	Saponite	Saponite/Poly(NIPAm): 11wt%.	Dispersion; Adsorption.	(Nakamura and Ogawa, 2013)
PS	Na- saponite	PS: 1.2 g in 100 ml water; Saponite content: 4–30 wt%; Co-stabilizer: hexadecane and AIBN.	Formation of asymmetric PS/saponite composite nanoparticles; Hydrophobically.	(Tong and Deng, 2013)

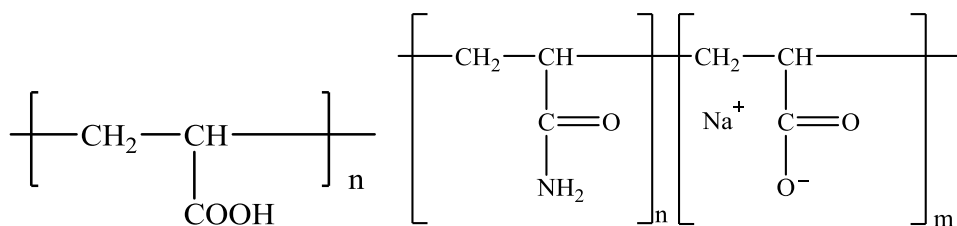
237 AM5/VP5C8Br: poly(acrylamide-co-(N-octyl-4-vinylpyridinium bromide))
 238 PAM: Polyacrylamide
 239 poly(NIPAm): poly(N-isopropylacrylamide);
 240 PS: polystyrene;
 241 RhPEG: rhodamine B (RhB) modified polyethylene glycol (PEG);
 242 xylan-METAC: xylan-2-(methacryloyloxyethyl) trimethyl ammonium chloride
 243

244 3. Anionic polyelectrolytes

245 3.1 Montmorillonite

246 Anionic polyelectrolytes are bearing negatively charged functional groups, commonly $-\text{COO}^-$,
 247 $-\text{O}-\text{SO}_3^{2-}$, $-\text{SO}_3^{2-}$, $-\text{O}-\text{CS}^{2-}$, $-\text{O}-\text{PO}_3^{2-}$, $-\text{PO}_3^{2-}$. The interaction between smectites and anionic
 248 polyelectrolytes seems impossible as both entities are bearing negatives charges. Yet researchers
 249 have explored that the interactions of smectite and anionic polyelectrolyte. The anionic
 250 polyelectrolyte includes copolymer of acrylamide, 2-acrylamido-2-methylpropane sulfonic acid
 251 (AM-AMPS) and a terpolymer of acrylamide, 2-acrylamido-2-methylpropane sulfonic acid, and
 252 N-Vinylpyrrolidone (AM-AMPS-NVP) (Ahmad et al., 2018), anionic polyacrylamide (APAM)
 253 (Heller and Keren, 2002), sulfonated polyacrylamide (SPA) (Oliyaei et al., 2015), anionic
 254 polyacrylamide–acrylate copolymer (Mpofu et al., 2004) (**Fig. 6**). The interactions can be divided
 255 into two types: an electrostatic interaction between the anionic polyelectrolyte chains and the
 256 positive charges on the edges of the smectite particles; a repulsive interaction between the
 257 negative smectite charge and the polyelectrolytes (Gumfekar and Soares, 2018). The
 258 smectite-anionic polyelectrolyte interactions in aqueous dispersion depend on molecular weight,
 259 polyelectrolyte concentration, size, surface charge and concentration of the smectite particles in
 260 water (Shaikh et al., 2017b).

261



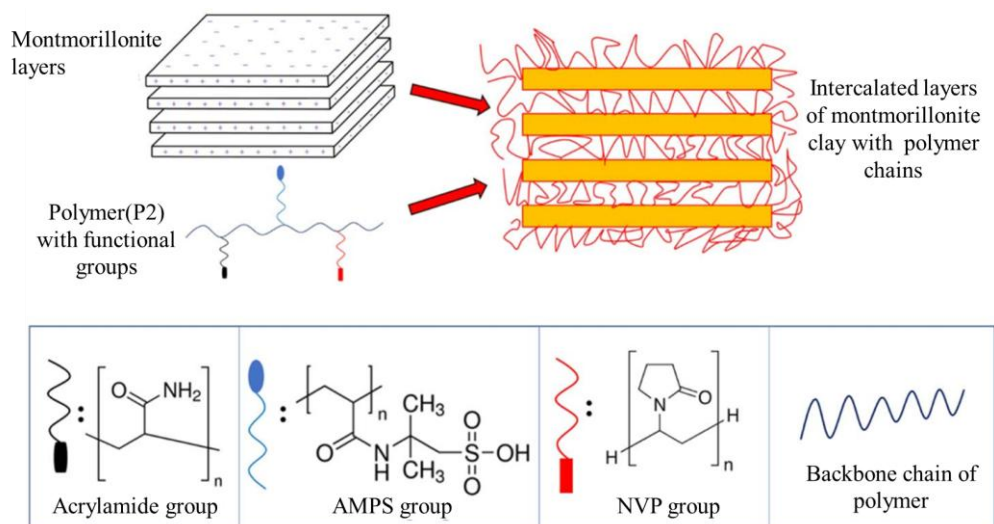
262

263

(a) Poly(acrylic acid)

(b) polyacrylamide (Ewanek, 2008)

283 (AM-AMPS) (P1) and a terpolymer of acrylamide, 2-acrylamido-2-methylpropane sulfonic acid,
 284 and N-vinylpyrrolidone (AM-AMPS-NVP (P2)) into aqueous montmorillonite dispersion can
 285 enhanced their rheological properties (viscosity and shear stress). The montmorillonite/polymer
 286 dispersions has higher viscosity and shear stress compared to the montmorillonite dispersions at
 287 1/s shear rate at 25°C in deionized water (Ahmad et al., 2018). And the montmorillonite/P2
 288 dispersion has higher viscosity and shear stress compared to the montmorillonite/P1 dispersion at
 289 1/s shear rate at 25°C in deionized water. This is because the polymer P2 has three different
 290 moieties with negative charges along the backbone whereas the polymer P1 has two moieties with
 291 negative charges (**Fig.7**). Therefore, there were stronger electrostatic repulsive interactions
 292 between polymer P2 and montmorillonite layers than for polymer P1, this stronger electrostatic
 293 repulsion gives the montmorillonite/P2 dispersion better rheology. In addition, Chalah et al. (2018)
 294 shows addition of the anionic polyelectrolyte xanthan gum into the 5% aqueous montmorillonite
 295 dispersion increased the viscosity of the water-montmorillonite dispersion. These recent findings
 296 prove the rational usage of different types of anionic polyelectrolytes additives in water-based
 297 drilling muds.
 298



299
 300 Fig. 7. Schematic diagram of montmorillonite/Polymer (P2) interactions. Reprinted from (Ahmad et al., 2018),
 301 copyright (2018), with permission from Elsevier.
 302

303 High molecular weight and high degrees of hydrolysis of anionic PAM in aqueous
 304 montmorillonite dispersion could be more effective in stabilizing montmorillonite aggregate than
 305 those with lower molecular weight and degrees of hydrolysis (Heller and Keren, 2002). Three
 306 possibilities for the interaction between PAM and montmorillonite particles may existing: (i) by
 307 anion exchange between the surface hydroxyl group of the montmorillonite and the carboxyl
 308 anion of PAM; (ii) by hydrogen bonding between the surface hydroxyl group and C = O of the
 309 PAM; (iii) by making a bridge involving divalent ions derived from electrostatic forces. Güngör
 310 ((2001) found that in FT-IR spectra, PAM exhibit adsorption bands at 1660 and 3450 cm^{-1} (N-H,

311 strong bond), while PAM with Ca-montmorillonite and Na-montmorillonite shows additional
312 adsorption bands at 1653 and 3433 cm^{-1} which indicating that PAM molecules and montmorillonite
313 particles were interacting. The PAM molecule were loosely bound and interacts near the surface
314 and/or into the interlayers of the montmorillonite. The dominant electrostatic repulsions between
315 the anionic PAM functional groups and the negative surface charge of montmorillonite were
316 responsible for the lower adsorption affinity of anionic PAM towards montmorillonite particles
317 (Barany et al., 2009; Shaikh et al., 2017b). The same amounts of anionic PAM was added to the
318 aqueous Na-montmorillonite dispersion and the aqueous Ca-montmorillonite dispersion under the
319 same conditions (2% Ca- and Na- montmorillonite–water systems), the aqueous
320 Na-montmorillonite dispersion and the aqueous Ca-montmorillonite dispersion showed different
321 rheological behaviors (N. Güngör, 2001). The anionic PAM has a flocculation effect in the
322 aqueous Ca-montmorillonite dispersion whereas it has a de-flocculation effect in aqueous
323 Na-montmorillonite dispersion as Ca^{2+} has a strong tendency to form face/face contacts, which
324 can cause defects in the edge (+)/face (-) network that promote its fragmentation. In the absence of
325 Ca^{2+} , the “house of cards” would decompose at edge charge densities, so Ca^{2+} ions can help the
326 formation of bridging flocculation.

327 PAM/montmorillonite dispersion has important role in several industries, including paper,
328 water treatment, enhanced oil recovery and drilling (Khoshniyat et al., 2012). Sulfonated
329 polyacrylamide (SPA) has higher thermal stability than standard hydrolyzed PAM and is
330 commercially used as stabilizer in oil fields up to 120°C (Oliyaei et al., 2015). The stability of
331 aqueous Na-montmorillonite dispersions in the absence of SPA, were due to the electrostatic
332 interactions. The presence of SPA, modified the Na-montmorillonite particle–particle interactions
333 as few SPA chains can be adsorbed onto the Na-montmorillonite particles surface via hydrogen
334 bonds between the oxygen atoms of Na-montmorillonite and the protons of the amide groups of
335 SPA, resulting in steric stability. However, there were repulsion between the negative layers of
336 Na-montmorillonite and the anionic groups of SPA, therefore, the two interactions, adsorption and
337 repulsion, result in dispersion stability.

338 Earlier, anionic polyacrylamide–acrylate copolymer proved effective in flocculating
339 montmorillonite dispersions (Mpofu et al., 2004). Both montmorillonite particles and PAM
340 molecules are negatively charged (pH=7.5), and the main driving force for adsorption was
341 hydrogen bonding between the silanol and aluminol OH groups at the montmorillonite particle
342 surfaces, particularly the edge faces and the amide ($-\text{CONH}_2$) groups (Lewis base) of the
343 copolymer. The longer the length of the copolymer, the higher flocculation efficiency of the
344 montmorillonite dispersion. The concentration of the anionic polyacrylamide–acrylate copolymer
345 flocculant increases, the size of the particles decreases, and the affinity and adsorption density
346 increase. Hence, polyacrylamide–acrylate copolymer is normally used as a flocculant in industry
347 for montmorillonite dispersions.

348

349
350

Table 2
Recent typical studies on the interactions between smectites and anionic polyelectrolytes

Anionic polyelectrolytes	Type of smectite	Conditions	Interaction	References
PAM	Montmorillonite	PAM: 2.0% v/v; Montmorillonite: 100 ml; The system: pH 9.	Lower adsorption capacities; Floc sizes increased.	(Shaikh et al., 2017b)
AM-AMPS	Montmorillonite	Montmorillonite content: 5 wt%; AM-AMPS content: 0.25 wt%; Temperatures: 25°C, 85°C	Electrostatic repulsive forces; Enhanced the rheological properties.	(Ahmad et al., 2018)
AM-AMPS-NV P	Montmorillonite	Montmorillonite content: 5 wt%; AM-AMPS-NVP content: 0.25 wt%; Temperatures: 25°C, 85°C	Electrostatic repulsive forces; Enhanced the rheological properties.	(Ahmad et al., 2018)
SPA	Montmorillonite	Montmorillonite content: 0.5~3 wt%; SPA content: 0~0.4 wt%.	Increased the Z-average particle sizes.	(Oliyai et al., 2015)
SPA	Hectorite	----	Hydrogen bonding; Ionic interaction.	(Ehsan et al., 2017)
PAAS	Hectorite	Hectorite content: 10 wt%; PAAS content: 3.5 wt% ; Molecular mass: 2.3×10^5 ; Dispersant: 0.25 wt% TSPP;	Adsorbed.	(Takeno and Nakamura, 2019)

351
352
353
354
355
356

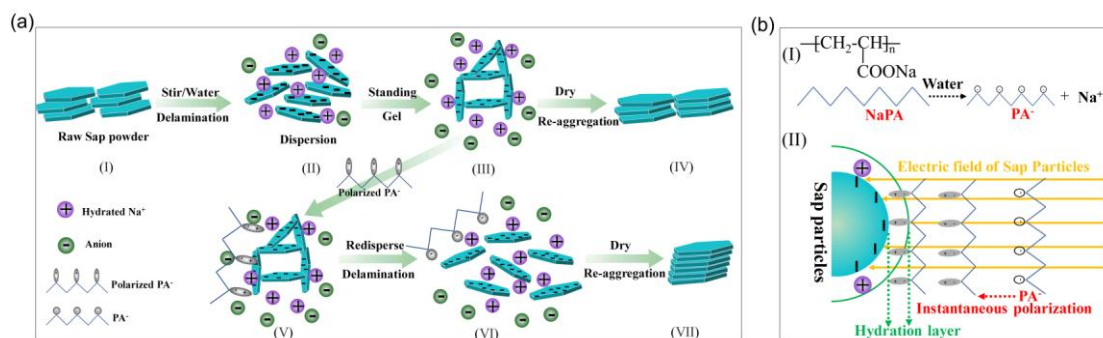
AM-AMPS: acrylamide and 2-acrylamido-2-methylpropane sulfonic acid
AM-AMPS-NVP: acrylamide, 2-acrylamido-2-methylpropane sulfonic acid, and N-Vinylpyrrolidone
PAM: Polyacrylamide
PAAS: Polyethylene oxide
SPA: Sulfonated polyacrylamide

357
358
359
360

3.2 Saponite and hectorite

Saponite can easily delaminate in water to form a sol or hydrogel and has been widely used in many products ranging in cosmetics, paints and adhesives (Zhou et al., 2019b). In most cases of formation of saponite sols or hydrogels, the key point is the interactions between saponite particles

361 and polyelectrolytes in their system. However, details on such interactions remain unclear. Li et al.
 362 (2019a) studied the rheological behaviors of saponite sol-gel system, and reveal the interaction
 363 between saponite particles and the sodium polyacrylate (NaPA) by preparing saponite hydrogels
 364 with polyelectrolyte NaPA (**Fig.8a**). It was found that the NaPA incorporated saponite hydrogel
 365 was transformed to a sol due to the destruction of the house-of-card structure, and the saponite
 366 was well dispersed (**Fig. 8aVI**). A possible mechanism was also reported to explain the
 367 transformation of saponite hydrogel to sol. Firstly, the PA⁻ instantaneous polarized in the electric
 368 field, which was formed near the saponite particles due to the surface charge. Then, it enters the
 369 saponite hydration layer to replace some of the original hydrated ions (Gong et al., 2018). Further,
 370 a strong chemical bond formed between the polarized PA⁻ and the saponite particles due to
 371 stronger electrostatic attraction (**Fig. 8bII**). They also found that the stacking order of saponite
 372 particles was promoted after drying from the saponite-NaPA dispersion (**Fig. 8aVII**). This work
 373 suggested interactions between saponite particles and polyacrylates which might provide a help to
 374 tune the rheological performance of saponite sol-gel products and explore more functional
 375 saponite-based nanomaterials (Del Gaudio et al., 2018).
 376



377
 378 Fig.8. (a) Schematic illustration of saponite dispersion with/without added NaPA and reaggregation after
 379 drying: (I) Saponite dispersed in water to form (II) Saponite dispersion and (III) Saponite hydrogel; (V) interaction
 380 of the saponite hydrogel with polarized PA to form (VI) Saponite NaPA dispersion; (IV) Saponite-control and (VII)
 381 Saponite-NaPA re-aggregated from Saponite hydrogel and Saponite-NaPA dispersion, respectively; (b) Illustrations
 382 of the interactions between saponite particles and NaPA: (I) Chemical formula of NaPA and schematic structure of
 383 NaPA; (II) interaction between aggregated saponite particle and NaPA. Reprinted with permission from (Li et al.,
 384 2019a). Copyright 2019 American Chemical Society.

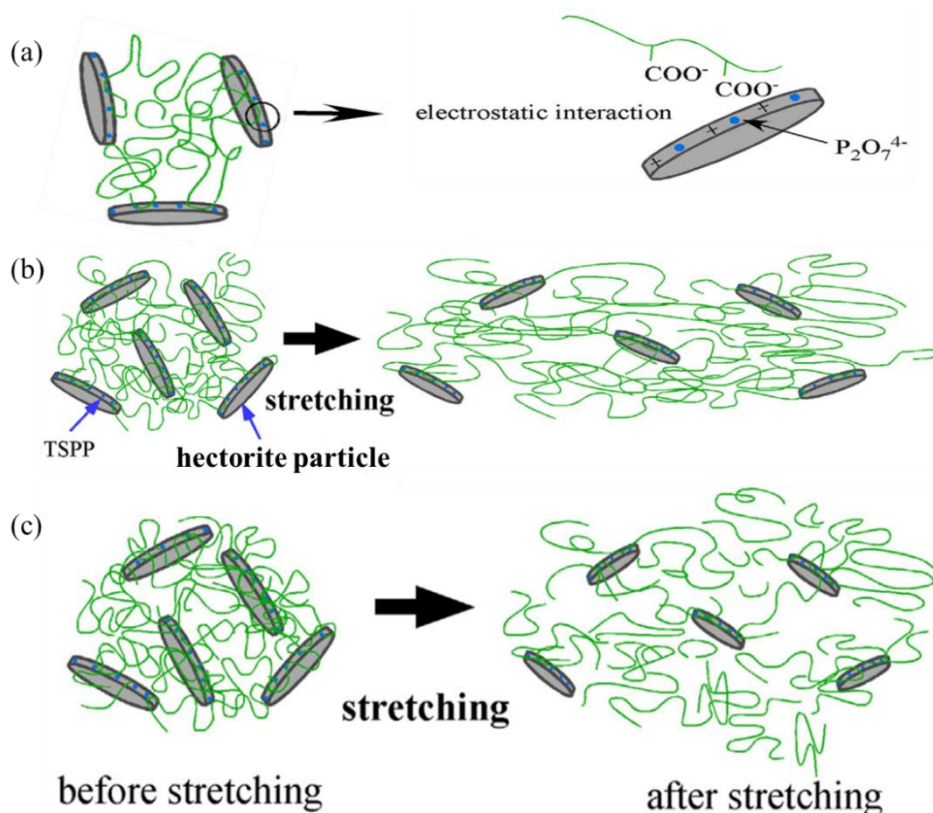
385

386 Hectorite, in particular the synthetic one, has been widely used in hydrogels (Du et al., 2016).
 387 In recent years, hydrogels with mechanical toughness have important application prospects in the
 388 fields of tissue engineering, health care, electronic skin, and soft robots, which have attracted great
 389 attention from researchers (Takeno and Nakamura, 2013; Takeno and Kimura, 2016; Takeno and
 390 Nakamura, 2019). Takeno and Kimura (2016) found that hydrogels prepared by simply blending
 391 an anionic NaPA with synthetic hectorite including a dispersant, tetrasodium pyrophosphate
 392 (TSPP), significantly improve the mechanical toughness of the resultant synthetic

393 hectorite/NaPA/TSPP gel. Due to the addition of TSPP, synthetic hectorite particles were
 394 homogeneously dispersed in the gel, since TSPP prevented formation of house-of-cards structure
 395 by adsorption of pyrophosphate anions onto the positively charged edge of hectorite particles (**Fig.**
 396 **9a**). Thus, the structural homogeneity in the hydrogel causes a significant increase of mechanical
 397 properties. In the case of anionic NaPA, carboxylate anion is also adsorbed on positively charged
 398 edge of synthetic hectorite particle (Takeno and Nakamura, 2013).

399 Molecular weight of NaPA in the synthetic hectorite/NaPA/TSPP gel system affects the
 400 tensile properties (Takeno and Kimura, 2016). Adding high molecular weight NaPA
 401 polyelectrolyte will improve the mechanical properties of hectorite / NaPA / TSPP gel system
 402 because the electrostatic interaction of high molecular weight NaPA with hectorite particles was
 403 stronger than for low molecular weight. In the case of the gel with high molecular weight NaPA,
 404 NaPA chains were capable of bridging adjacent synthetic hectorite particles. The long chain can
 405 keep cross-linking adjacent synthetic hectorite particles even under high elongation (**Fig.9b**).
 406 However, in the case of the gel with low molecular weight NaPA, when the gel was stretched, the
 407 short chains were not capable of bridging adjacent synthetic hectorite particles. Therefore, gel with
 408 low molecular weight NaPA has poor mechanical properties (**Fig.9c**). Hence, the use of high
 409 molecular weight polyelectrolytes is essential for producing blended hydrogels with mechanical
 410 toughness.

411



412

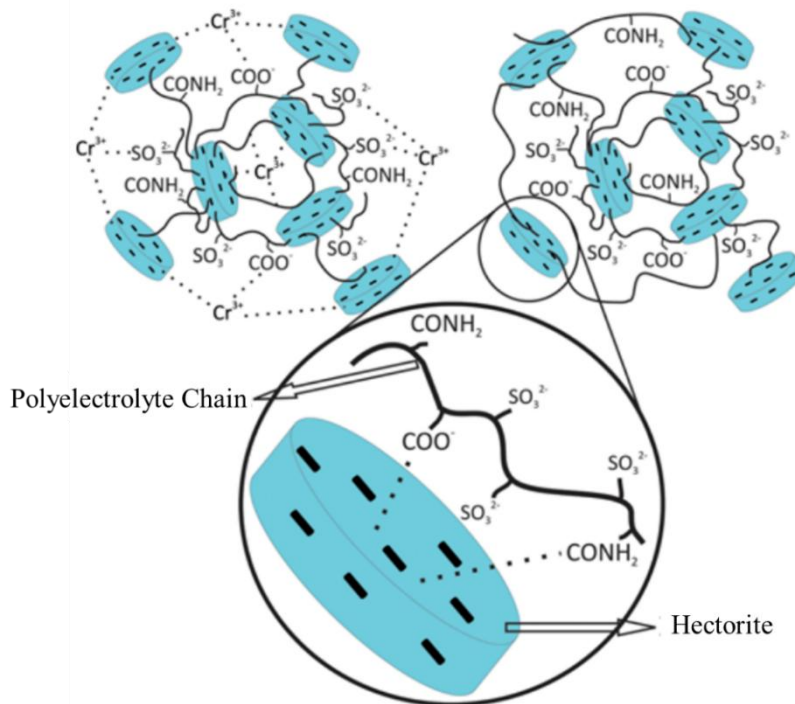
413 Fig.9 (a) A schematic representation of synthetic hectorite /NaPA/TSPP gel; and hydrogels composed of
 414 synthetic hectorite and NaPA with (b) high molecular weight ($3.50 \times 10^6 \leq Mw \leq 2.11 \times 10^7$) and (c) with low

415 molecular weight ($2.25 \times 10^5 \leq M_w \leq 1.55 \times 10^6$) before and after stretching. Reprinted from (Takeno and Kimura,
416 2016). Copyright (2016), with permission from Elsevier.

417

418 Synthetic hectorite is a multifunctional cross-linker helping polyelectrolyte form networks.
419 (Ehsan et al., 2017) prepared weak sulfonated polyacrylamide (SPA) nanocomposite hydrogels
420 using synthetic hectorite nanoparticles and/or Cr^{3+} as crosslinker in saline solution. The interaction
421 between the SPA and synthetic hectorite was a combination of hydrogen bonding and ionic
422 interaction. The interactions between SPA and synthetic hectorite as well as the formation of SPA/
423 synthetic hectorite systems and SPA/ Cr^{3+} / synthetic hectorite systems are shown in **Figure 10**. The
424 oxygen atoms on the synthetic hectorite surface with the amide proton of SPA may form hydrogen
425 bonds, and the metal atoms on the synthetic hectorite surface may form a complex with the
426 carboxylate oxygen of SPA (Li et al., 2008). Adsorption properties of SPA/ Cr^{3+} / synthetic hectorite
427 systems increased when synthetic hectorite concentration was increased. This phenomenon may
428 be due to the increased hydrogen bonding interaction of the amide group of the SPA with Si-OH
429 and Si-O-Si groups, or ionic interaction of the synthetic hectorite surface (Abdurrahmanoglu and
430 Okay, 2010). Both SPA/ Cr^{3+} /synthetic hectorite systems and SPA/synthetic hectorite systems
431 interactions increased the storage modulus. The SPA crosslinked with Cr^{3+} and synthetic hectorite
432 nanocomposite hydrogel exhibited better viscoelastic behavior than SPA polyelectrolyte or
433 SPA/ Cr^{3+} hydrogels. Therefore, SPA/ Cr^{3+} / synthetic hectorite systems may be a potential option
434 for field applications in hostile conditions due to better viscoelasticity and adsorption.

435



436

437 Fig.10 Schematic drawings of the formation of SPA/hectorite and SPA/ Cr^{3+} /hectorite hydrogels. Reprinted by
438 permission from Springer Nature: Springer (Ehsan et al., 2017). Copyright 2017.

439

440 **4. Amphoteric polyelectrolytes**

441 **4.1 Montmorillonite**

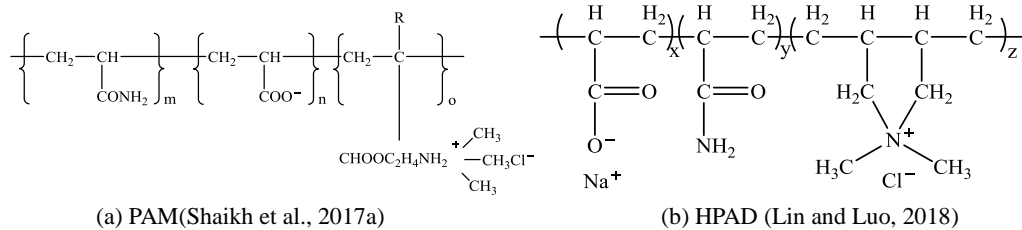
442 An amphoteric polyelectrolyte has both cationic and anionic groups distributed along the
443 carbon chain. The solubility of amphoteric polyelectrolytes in water depends on the charge density,
444 charge balance, asymmetry, and the chemical nature of the ionizable groups (Rabiee et al., 2014).
445 The polymer bridging, charge neutralization, and polymer adsorption (Song et al., 2010) between
446 the smectite and amphoteric polyelectrolytes promote flocculation in aqueous smectite-amphoteric
447 polyelectrolytes dispersion, so amphoteric polyelectrolyte has been used in water treatment (Wang
448 et al., 2019), and drilling fluid (Bai et al., 2015; Chu et al., 2013) (**Table 3**).

449 Gelatin, a natural amphoteric polyelectrolyte, due to biocompatibility, biodegradable
450 properties, and no toxicity and availability, can potentially be a suitable substitute for the existing
451 flocculants (Karimi et al., 2013). Gelatin can be effectively adsorbed on montmorillonite surfaces
452 thereby changing the electrochemical nature of montmorillonite particle surface changes
453 (Nazarzadeh et al., 2017). The adsorbed gelatin chains introduce bridging forces and steric forces
454 in addition to electrostatic repulsion and Van der Waals attraction. In addition, the range of
455 montmorillonite particle-particle interactions will also change with the thickness of the adsorbed
456 layer, especially tail length of gelatin chains in the aqueous montmorillonite dispersion.
457 Nevertheless, gelatin chains including cationic, anionic and uncharged monomer residues, the
458 adsorption depends on the Coulomb interaction between the net charge on the carbon chain and
459 the charged surface of montmorillonite (Kudaibergenov and Ciferri, 2007). If the excess charge on
460 the gelatin chain is same as the charges of the montmorillonite surface, the Coulomb repulsion
461 may inhibit adsorption. If the excess charges on the gelatin chain are opposite to those of the
462 charges of the montmorillonite surface, the Coulomb interaction may promote adsorption.

463 Because amphoteric polyelectrolyte has both cationic and anionic groups distributed along
464 the carbon chain, the content of anions and cations are needed to achieve specific purpose can be
465 adjusted. For example, based on the ratio of cationic and anionic groups on the chains, amphoteric
466 polyacrylamides exhibited variable flocculation efficiencies (Shaikh et al., 2017b) (**Fig.11a**).
467 Polyacrylamides with a high ratio of cationic groups/anionic groups clearly displayed cationic
468 behavior with high removal efficiency, while poor flocculation capabilities were observed with a
469 low ratio of cationic-groups/anionic-groups. Hydrolyzed poly(acrylamide/dimethyl diallyl
470 ammonium chloride) (HPAD), a polyampholyte containing quaternary ammonium groups,
471 carboxylic acids, and amides has high ratio of cationic quaternary ammonium groups and specific
472 carboxylic acids, and amides (Lin and Luo, 2018) (**Fig.11b**). The addition of HPAD amphoteric
473 polyelectrolyte to the aqueous montmorillonite dispersion results in a strong electrostatic
474 interaction between the charged chemical groups (quaternary ammonium groups, carboxylic acids,
475 and amides) and montmorillonite particles, thus causing the formation of HPAD polymer bridges
476 between adjacent montmorillonite particles and enlarges the charge imbalance of montmorillonite

477 (Liu et al., 2016). Therefore, by introducing electrostatic repulsion, the HPAD helped
 478 montmorillonite maintain a broad particle size distribution. In return, broad particle size
 479 distribution contributed to the adsorption of HPAD on montmorillonite. Optimization of the
 480 composition of amphoteric polyelectrolyte could be useful for the future design and synthesis of
 481 filtration reducers in the oil and gas field.

482



485

Fig.11. Chemical structures of the non-ionic polyelectrolytes

486

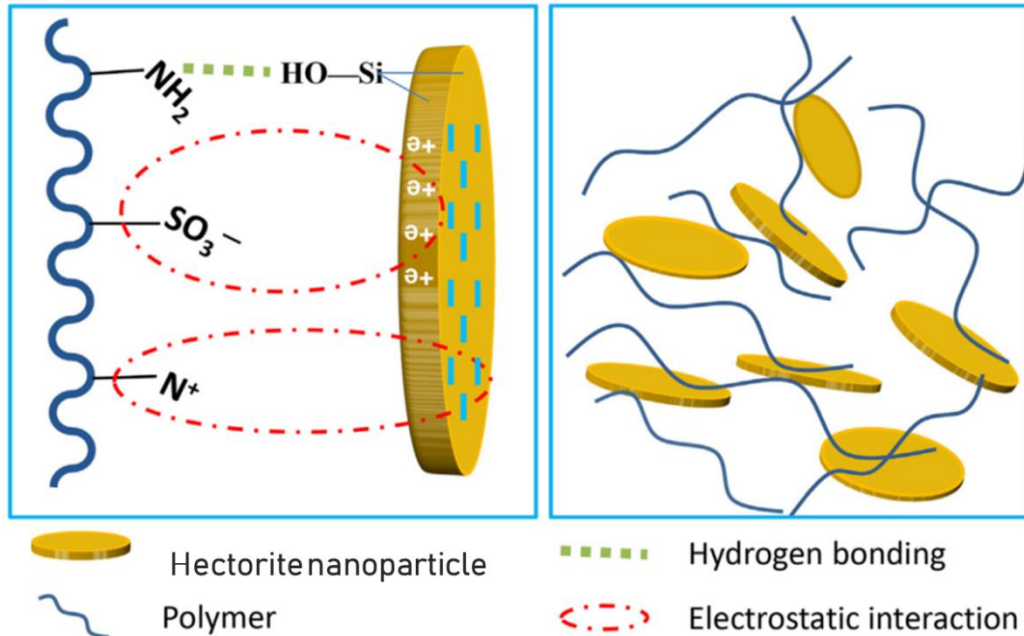
487 4.2 Saponite and hectorite

488 The amphoteric polyelectrolyte can interact with saponite. In saponite–cationic PAM–anionic
 489 PAM–water mixtures, the cationic PAM was first adsorbed on the saponite particles by
 490 electrostatic and hydrogen bonding (Zhang et al., 2005). Then, the anionic PAM was adsorbed on
 491 the saponite particles by electrostatic or Van der Waals forces. The PAM molecule crosslinks with
 492 the cationic PAM adsorbed on the saponite particles in saponite aqueous solution to form a spatial
 493 network. The viscosity of the saponite–cationic PAM–anionic PAM–water mixtures was increased
 494 due to the interaction between anionic PAM and cationic PAM. Under the shear force, the spatial
 495 network was gradually destroyed. The structure can be reformed again when rested for a while due
 496 to thixotropy. This system can be used as an excellent water blocking agent for oil layers with
 497 large pores and high permeability.

498 Interaction between hectorite and amphoteric polyelectrolytes can improve the thermal
 499 stability of the drilling fluid. Huang et al. (2019) studied the interaction between hectorite and a
 500 terpolymer (AAD) by synthesizing through radical polymerization of acrylamide,
 501 2-acrylamido-2-methylpropane sulfonic acid, and diallyldimethylammonium chloride monomers.
 502 The disk-shaped synthetic hectorite nanoparticles was well dispersed in aqueous terpolymer AAD
 503 dispersion, and the hectorite nanoparticles were establishing strong interactions between
 504 terpolymer AAD. The interactions included (**Fig. 12**): 1) electrostatic attractions between
 505 negatively charged synthetic hectorite surfaces and quaternary ammonium cationic groups of
 506 terpolymer AAD; 2) electrostatic attractions between positively charged synthetic hectorite edges
 507 and negatively charged sulfate groups of terpolymer AAD; and 3) possible hydrogen bonding
 508 between hydroxyl groups of synthetic hectorite and amide groups of terpolymer AAD. The
 509 interactions reduced the mobility of terpolymer AAD chains and also slowed down the
 510 degradation. This hectorite-terpolymer AAD system can increase the viscosity of drilling fluids.
 511 Synthetic hectorite could substantially improve the thermal stability of drilling fluid by protecting

512 terpolymer AAD. This interactions between synthetic hectorite nanoparticles and amphoteric
 513 polyelectrolytes provided a novel strategy to develop high temperature-resistant drilling fluids for
 514 deep reservoir excavation (Akhtarmanesh et al., 2013; Li et al., 2015).

515



516

517 Fig.12 The proposed mechanism of the interactions between synthetic hectorite nanoparticles and terpolymer
 518 ADD. Reprinted from (Huang et al., 2019). Copyright 2019, with permission from Elsevier.

519

520 Table 3

521 Recent typical studies on the interaction between smectite and amphoteric polyelectrolytes.

Amphoteric polyelectrolytes.	Type of smectite	Conditions	Interaction	References
HPAD	Montmorillonite	HPAD:0.5-2 wt%; Montmorillonite: 5wt%; Na ₂ SO ₃ :0.25 wt%; pH 8.	Adsorption; Introducing electrostatic repulsion and entropic repulsion.	(Lin and Luo, 2018)
PAM	Montmorillonite	PAM: 2.0% v/v; Montmorillonite: 100 ml; The system: pH 9.	Lower adsorption capacities due to steric hindrance.	(Shaikh et al., 2017b)
PECT/CS	Montmorillonite	PECT/CS ratios: 1:1, 1:2 and 2:1; Montmorillonite concentration: 0.5 and 2% wt.	Novel nanocomposite hydrogels were produced; Increased the degree of swelling and the mechanical resistance.	(da Costa et al., 2016)
ADD	Synthetic hectorite	AAD: 1-2 g; Synthetic hectorite:2 wt%; pH 7.	Electrostatic attractions; Hydrogen bonding; Rheological.	(Huang et al., 2019)

522 ADD: acrylamide, 2- acrylamido-2-methylpropane sulfonic acid, and diallyldimethylammonium chloride
 523 monomers

524 HPAD: Hydrolyzed poly(acrylamide/dimethyl diallyl ammonium chloride)

525 PAM: Polyacrylamide

526 PECT/CS: pectin/chitosan

527

528 Generally, for cationic polyelectrolytes, they are adsorbed onto the smectite surface through
529 hydrogen bonding interactions between the Si-OH and Al-OH groups and functional group of
530 polyelectrolyte's (Nasser et al., 2013). Cationic polyelectrolytes can also interact with the smectite
531 through ion exchange by the electrostatic attraction between the positively charged cationic
532 polyelectrolytes and the negatively charged smectite. By contrast, electrostatic repulsion occurs
533 between anionic polyelectrolytes and smectite surfaces because both carry the negative charge.
534 The electrostatic repulsion weakens the adsorption of smectite by anionic polyelectrolytes, thereby
535 reducing the adsorption capacity. It also interacts with the smectite through van der Waals and
536 possibly by H-bonding. Amphoteric polyelectrolytes exhibit both cationic polyelectrolytes and
537 anionic polyelectrolytes behavior and their adsorption capacities are in between the cationic and
538 anionic polyelectrolytes. Under the same conditions, for the same polyelectrolyte with different
539 surface charge types, the adsorption affinity of smectite surface are easier and stronger for
540 polyelectrolytes in the order: cationic polyelectrolytes > amphoteric polyelectrolytes > anionic
541 polyelectrolytes (Shaikh et al., 2017).

542

543 **5. Concluding remarks and future work**

544 Recent studies have significantly deepened the understanding of the interactions between
545 smectites and polyelectrolytes. The polyelectrolytes contribute to the adsorption, flocculation and
546 rheological behavior of aqueous smectite dispersion. It is expected that the use of such
547 polyelectrolytes with smectites will enhances the smectite processing, separations and waste water
548 treatment and oil well drilling fluid.

549 It is now known that different types of polyelectrolytes and type of smectite along with
550 polyelectrolyte molecular weight, charge type and charge density affect the interactions between
551 smectite and polyelectrolyte. Although great progress has been made but scientific knowledge of
552 the role of interactions between smectite and polyelectrolyte is still in its infancy. Most of the
553 current research on smectite and polyelectrolyte interactions has so far been concerned with
554 montmorillonite and fewer studies exist on the interaction between polyelectrolytes and saponite
555 or hectorite. In addition, the species of polyelectrolytes are numerous but only a few types have
556 been investigated for their interactions with smectites. The accurate experimental evidence on the
557 hydrogen bonding, hydrophobic interaction, ion binding, electrostatic interaction, and van der
558 Waals forces are limited. In particular, no quantitative data and reliable equations have been
559 established. Hence, the detailed models and mechanisms at the molecular or atomic level remain
560 unclear.

561 Moreover, it needs to be mentioned that interactions between smectite and polyelectrolyte in
562 wastewater treatment was mostly conducted at laboratory scale. Wastewater treatment by

563 adsorption, flocculation and separation on an industrial scale is still a challenge. Desirable
564 polyelectrolytes as flocculants and smectite should be economically able to provide enough
565 removal efficiency for pollutants in wastewaters under a wide range of conditions. Meanwhile, the
566 polyelectrolyte and the process should be environmentally friendly, cost-effective and easily
567 reproducible.

568 The interaction between smectites and polyelectrolytes get conventionally involved in using
569 smectite-polyelectrolyte system as adsorbent, flocculant, rheological additives. Some studies have
570 demonstrated new applications in biomaterial, three-dimensional (3D) printable ink materials and
571 sensor devices by taking advantage of the interaction of smectites with polyelectrolytes. The
572 smectite-based nanocomposites and hierarchical materials can be fabricated by the surface
573 engineering and tactic assembly of smectites. Interactions between smectites and polyelectrolytes
574 can result in the formation of nanohybrids as biosensors, catalysts and drug carriers. In-depth
575 understanding of the interaction between polyelectrolytes and smectites also helps expanding the
576 integration and functionality and inherent mechanism of advanced smectite-polyelectrolyte
577 materials.

578

579 **Acknowledgements**

580 The authors wish to acknowledge financial support from the National Natural Scientific Foundation of China (41672033), the
581 Zhejiang 151 Talents Project, The State Key Laboratory Breeding Base of Green Chemistry-Synthesis Technology, The Zhejiang
582 University of Technology (GCTKF2014006), Key Laboratory of Clay Minerals of Ministry of Land and Resources of the People's
583 Republic of China, Engineering Research Center of Non-metallic Minerals of Zhejiang Province, Zhejiang Institute of Geology and
584 Mineral Resource, Hangzhou 310007, China (ZD2018K04).

585

- 587 Aalaie, J., 2012. Rheological Behavior of Polyacrylamide/Laponite Nanoparticle Suspensions in
588 Electrolyte Media *J. Macromol. Sci. B.* 51(6), 1139-1147.
- 589 Abdurrahmanoglu, S., Okay, O., 2010. Rheological behavior of polymer-clay nanocomposite
590 hydrogels: Effect of nanoscale interactions. *J. Appl. Polym. Sci.* 116(4), 2328-2335.
- 591 Abu-Jdayil, B., 2011. Rheology of sodium and calcium bentonite–water dispersions: Effect of
592 electrolytes and aging time. *Int. J. Miner. Process.* 98(3-4): 208-213.
- 593 Ahmad, H.M., Kamal, M.S., Al-Harhi, M.A., 2018. Rheological and filtration properties of
594 clay-polymer systems: Impact of polymer structure. *Appl. Clay. Sci.* 160: 226-237.
- 595 Akhtarmanesh, S., Shahrabi, M.A., Atashnezhad, A., 2013. Improvement of wellbore stability in
596 shale using nanoparticles. *J. Petrol. Sci. Eng.* 112: 290-295.
- 597 Alemdar, A., Bütün, V., 2005. Interaction between a tertiary amine methacrylate based
598 polyelectrolyte and a sodium montmorillonite dispersion and its rheological and colloidal
599 properties. *J. Appl. Polym. Sci.* 95(2): 300-306.
- 600 Alemdar, A., Öztekin, N., Erim, F., Ece, Ö., Güngör, N., 2005. Effects of polyethyleneimine
601 adsorption on rheology of bentonite suspensions. *B. Mater. Sci.* 28(3): 287-291.
- 602 Aydin, M., Uyar, T., Tasdelen, M.A., Yagci, Y., 2015. Polymer/clay nanocomposites through
603 multiple hydrogen-bonding interactions. *J. Polym. Sci. A. Polym. Chem.* 53(5): 650-658.
- 604 Bai, X., Yang, Y., Xiao, D., Pu, X., Wang, X., 2015. Synthesis, characterization, and performance
605 evaluation of the AM/AMPS/DMDAAC/SSS quadripolymer as a fluid loss additive for
606 water-based drilling fluid. *J. Appl. Polym. Sci.* 132(14).
- 607 Bandla, M., Abbavaram, B.R., Kokkarachedu, V., Sadiku, R.E., 2017. Silver nanoparticles
608 incorporated within intercalated clay/polymer nanocomposite hydrogels for antibacterial
609 studies. *Polym. Composite.* 38: 16-23.
- 610 Barany, S., Meszaros, R., Kozakova, I., Skvarla, I., 2009. Kinetics and mechanism of flocculation
611 of bentonite and kaolin suspensions with polyelectrolytes and the strength of floccs.
612 *Colloid. j.* 71(3): 285-292.
- 613 Beisebekov, M.M., Serikpayeva, S.B., Zhmagalieva, S.N., Beisebekov, M.K., Abilov, Z.A.,
614 Kosmella, S., Koetz, J., 2014. Interactions of bentonite clay in composite gels of
615 non-ionic polymers with cationic surfactants and heavy metal ions. *Colloid. Polym. Sci.*
616 293(2): 633-639.
- 617 Bergaya, F., Lagaly, G., 2013. General Introduction, Handbook of Clay Science. *Dev. Clay. Sci.*
618 1-19.
- 619 Blachier, C., Michot, L., Bihannic, I., Barres, O., Jacquet, A., Mosquet, M., 2009. Adsorption of
620 polyamine on clay minerals. *J. Colloid. Interface. Sci.* 336(2): 599-606.
- 621 Budnyak, T.M., Yanovska, E.S., Kichkiruk, O.Y., Sternik, D., Tertykh, V.A., 2016. Natural
622 Minerals Coated by Biopolymer Chitosan: Synthesis, Physicochemical, and Adsorption
623 Properties. *Nanoscale. Res. Lett.* 11(492): 1-12.
- 624 Campos, V., Tcacenco, C.M., 2015. Synthesis of polycationic bentonite-ionene complexes and
625 their benzene adsorption capacity. *Polímeros.* 25(2): 146-153.
- 626 Carli, L.N., Daitx, T.S., Guegan, R., Giovanela, M., Crespo, J.S., Mauler, R.S., 2015. Biopolymer
627 nanocomposites based on poly(hydroxybutyrate-co-hydroxyvalerate) reinforced by a
628 non-ionic organoclay. *Polymer International.* 64(2): 235-241.

629 Chalah, K., Benmounah, A., Benyounes, K., 2018. Effect of anionic polyelectrolytes on the flow
630 of activated sodium bentonite drilling mud. *Matec. Web. Conf. Edp. Sci.* 01082.

631 Chu, Q., Luo, P., Zhao, Q., Feng, J., Kuang, X., Wang, D., 2013. Application of a new family of
632 organosilicon quadripolymer as a fluid loss additive for drilling fluid at high temperature.
633 *J. Appl. Polym. Sci.* 128(1): 28-40.

634 Craciun, G., Ighigeanu, D., Manaila, E., Stelescu, M.D., 2015. Synthesis and characterization of
635 poly (acrylamide-co-acrylic acid) flocculant obtained by electron beam irradiation. *Mater.*
636 *Res.* 18(5): 984-993.

637 da Costa, M.P., de Mello Ferreira, I.L., de Macedo Cruz, M.T., 2016. New polyelectrolyte
638 complex from pectin/chitosan and montmorillonite clay. *Carbohydr. Polym.* 146: 123-30.

639 Dawson, J.I., Oreffo, R.O., 2013. Clay: new opportunities for tissue regeneration and biomaterial
640 design. *Advanced Materials.* 25(30): 4069-86.

641 de Figueiredo, J.M.R., Araujo, J.P., Silva, I.A., Cartaxo, J.M., Neves, G.A., Ferreira, H.C., 2014.
642 Purified Smectite Clays Organofilized with Ionic Surfactant for Use in Oil-based Drilling
643 Fluids. In: S.M. Castanho, W. Acchar and D. Hotza (Editors), *Brazilian Ceramic*
644 *Conference 57. Materials Science Forum.* 21-26.

645 de Souza, G.S., Luporini, S., Rigoli, I.C., 2017. Rheological characterization of saline clay
646 dispersions with xanthan gum for oil well drilling fluids. *Materia-Brazil.* 22(1): 11796.

647 Del Gaudio, V., Luo, Y., Wang, Y., Wasowski, J., 2018. Using ambient noise to characterise
648 seismic slope response: The case of Qiaozhuang peri-urban hillslopes (Sichuan, China).
649 *Eng. Geol.* 246: 374-390.

650 Diouri, A., Chalah, K., Benmounah, A., Benyounes, K., Boukhari, A., Ait Brahim, L., Bahi, L.,
651 Khachani, N., Saadi, M., Aride, J., Nounah, A., 2018. Effect of anionic polyelectrolytes
652 on the flow of activated sodium bentonite drilling mud. *Matec. Web. Conf.* 149.

653 Du, Z.S., Hu, Y., Gu, X.Y., Hu, M., Wang, C.Y., 2016. Poly(acrylamide) microgel-reinforced
654 poly(acrylamide)/hectorite nanocomposite hydrogels. *Colloid. Surface. A.* 489: 1-8.

655 Ehsan, A., Jamal, A., Mahmood, H., Ahmad, S.V., 2017. Thermal stability, adsorption and
656 rheological behaviors of sulfonated polyacrylamide/chromium triacetate/laponite
657 nanocomposite weak gels. *Macromol. Res.* 25(1): 27-37.

658 Ewanek, J., 2008. *Water-Based Polymer Drilling Fluid and Method of Use.* US.

659 Falode, O., Ehinola, O., Nebeife, P., 2008. Evaluation of local bentonitic clay as oil well drilling
660 fluids in Nigeria. *Appl. Clay. Sci.* 39(1-2): 19-27.

661 Gong, Y., Tian, R., Li, H., 2018. Coupling effects of surface charges, adsorbed counterions and
662 particle-size distribution on soil water infiltration and transport. *Eur. J. Soil. Sci.* 69(6):
663 1008-1017.

664 Gumfekar, S.P., Soares, J.B.P., 2018. A novel hydrophobically-modified polyelectrolyte for
665 enhanced dewatering of clay suspension. *Chemosphere.* 194: 422-431.

666 Hasan, A., Fatehi, P., 2018. Cationic kraft lignin-acrylamide as a flocculant for clay suspensions: 1.
667 Molecular weight effect. *Sep. Purif. Technol.* 207: 213-221.

668 Hasan, A., Fatehi, P., 2019. Cationic kraft lignin-acrylamide copolymer as a flocculant for clay
669 suspensions: (2) Charge density effect. *Sep. Purif. Technol.* 210: 963-972.

670 Heller, H., Keren, R., 2002. Anionic Polyacrylamide Polymers Effect on Rheological Behavior of
671 Sodium-Montmorillonite Suspensions. *Soil. Sci. Soc. Am. J.* 66(1): 19-25.

672 Huang, X., Lv, K., Sun, J., Lu, Z., Bai, Y., Shen, H., Wang, J., 2019. Enhancement of thermal
673 stability of drilling fluid using laponite nanoparticles under extreme temperature
674 conditions. *Mater. Lett.* 248: 146-149.

675 Ismadji, S., Soetaredjo, F.E., Ayucitra, A., 2015. Natural Clay Minerals as Environmental Cleaning
676 Agents, Clay Materials for Environmental Remediation. *SpringerBriefs in Molecular
677 Science.* 5-37.

678 Kafashi, S., Rasaei, M., Karimi, G., 2017. Effects of sugarcane and polyanionic cellulose on
679 rheological properties of drilling mud: an experimental approach. *Egy. J. Petro.* 126(2):
680 371-374.

681 Karagüzel, C., Çetinel, T., Boylu, F., Çinku, K., Çelik, M., 2010. Activation of (Na, Ca)-bentonites
682 with soda and MgO and their utilization as drilling mud. *Appl. Clay. Sci.* 48(3): 398-404.

683 Karimi, F., Qazvini, N.T., Namivandi-Zangeneh, R., 2013. Fish gelatin/laponite biohybrid elastic
684 coacervates: A complexation kinetics–structure relationship study. *Int. J. Bbiol. Macromol.*
685 61: 102-113.

686 Kelessidis, V.C., Zografou, M., Chatzistamou, V., 2013. Optimization of drilling fluid rheological
687 and fluid loss properties utilizing PHPA polymer. *Soc. Petrole. Eng.*

688 Khoshniyat, A., Hashemi, A., Sharif, A., Aalaie, J., Duobis, C., 2012. Effect of surface
689 modification of bentonite nanoclay with polymers on its stability in an electrolyte solution.
690 *Polym. Sci. Ser. B.* 54(1-2): 61-72.

691 Kim, U., Carty, W.M., 2016. Effect of polymer molecular weight on adsorption and suspension
692 rheology. *J. Ceram. Soc. Jap.* 124(4): 484-488.

693 Kudaibergenov, S.E., Ciferri, A., 2007. Natural and Synthetic Polyampholytes, 2: Functions and
694 Applications. *Macromol. Rapid. Comm.* 28(20): 1969-1986.

695 Lee, C.S., Robinson, J., Chong, M.F., 2014. A review on application of flocculants in wastewater
696 treatment. *Process. Saf. Environ.* 92(6): 489-508.

697 Li, C., Wu, Q., Petit, S., Gates, W.P., Yang, H., Yu, W., Zhou, C., 2019a. Insights into the
698 Rheological Behavior of Aqueous Dispersions of Synthetic Saponite: Effects of Saponite
699 Composition and Sodium Polyacrylate. *Langmuir.* 35(40): 13040-13052.

700 Li, M., Wu, Q., Song, K., Qing, Y. and Wu, Y., 2015. Cellulose nanoparticles as modifiers for
701 rheology and fluid loss in bentonite water-based fluids. *Appl. Mater. Interface.* 7:
702 5006–5016.

703 Li, P., Kim, N.H., Heo, S.-B., Lee, J.-H., 2008. Novel PAAm/Laponite clay nanocomposite
704 hydrogels with improved cationic dye adsorption behavior. *Compos. Part. B-Eng.* 39(5):
705 756-763.

706 Lin, L., Luo, P., 2018. Effect of polyampholyte-bentonite interactions on the properties of
707 saltwater mud. *Appl. Clay. Sci.* 163: 10-19.

708 Liu, F., Jiang, G., Peng, S., He, Y., Wang, J., 2016. Amphoteric polymer as an anti-calcium
709 contamination fluid-loss additive in water-based drilling fluids. *Energ. Fuel.* 30(9):
710 7221-7228.

711 Mansri, A., Hocine, T., Bouras, B., Ben-habib, K., 2019. Synthesis of a new flocculant based on
712 poly(acrylamide-co-(N-octyl-4-vinylpyridinium bromide)) [AM5/VP5C8Br]-application
713 for the turbidity removal from clay suspension. *J. Macromol. Sci. A.* 56(1): 96-103.

714 Marchuk, S., Churchman, J., Rengasamy, P., 2016. Possible effects of irrigation with wastewater
715 on the clay mineralogy of some Australian clayey soils: laboratory study. *Soil. Res.*54(7):
716 857-868.

717 Mishchenko, M., Ozheredov, I., Postnova, I., Sapozhnikov, D., Shkurinov, A., Shchipunov, Y.A.,
718 2016. A terahertz spectroscopic study of chitosan-based bionanocomposites containing
719 clay nanoparticles. *Colloid J.* 78(2): 189-195.

720 Mpofu, P., Addai-Mensah, J., Ralston, J., 2004. Flocculation and dewatering behaviour of smectite
721 dispersions: effect of polymer structure type. *Miner. Eng.* 17(3): 411-423.

722 N. Güngör, S.K.I., 2001. Interactions of polyacrylamide polymer with bentonite in aqueous
723 systems. *Mater. Lett.* 48: 168–175.

724 Nakamura, T., Ogawa, M., 2013. Adsorption of cationic dyes within spherical particles of
725 poly(N-isopropylacrylamide) hydrogel containing smectite. *Appl. Clay. Sci.* 83-84:
726 469-473.

727 Nazarzadeh, M., Nikfarjam, N., Qazvini, N.T., 2017. Flocculation properties of a natural
728 polyampholyte: The optimum condition toward clay suspensions. *Environ. Eng. Res.*
729 22(3): 255-265.

730 Nasser, M., Twaiq, F., Onaizi, S.A., 2013. Effect of polyelectrolytes on the degree of flocculation
731 of papermaking suspensions. *Sep. Purif. Technol.* 103: 43–52.

732 Oliyaei, N., Aalaie, J., Barati, A., Miri, T., 2015. Study on Steady Shear Rheological Behavior of
733 Concentrated Suspensions of Sulfonated Polyacrylamide/Na-Montmorillonite
734 Nanoparticles. *J. Macromol. Sci. B.* 54(7): 761-770.

735 Oztekin, N., 2017. Removal of sodium dodecylbenzenesulfonate from aqueous solution using
736 polyethyleneimine-modified bentonite clay. *Desalin. Water. Treat.* 80: 268-275.

737 Petzold, G., Schwarz, S., 2013. Polyelectrolyte complexes in flocculation applications. *Adv.*
738 *Polym. Sci.* 256: 25-65.

739 Postnova, I., Sarin, S., Silant'ev, V., Ha, C.-S., Shchipunov, Y., 2015. Chitosan bionanocomposites
740 prepared in the self-organized regime. *Pure. Appl. Chem.* 87(8): 793-803.

741 Rabiee, A., Ershad-Langroudi, A., Jamshidi, H., 2014. Polyacrylamide-based polyampholytes and
742 their applications. *Rev. Chem. Eng.*30(5): 501-519.

743 Sakhawoth, Y., Michot, L.J., Levitz, P., Malikova, N., 2017. Flocculation of Clay Colloids Induced
744 by Model Polyelectrolytes: Effects of Relative Charge Density and Size. *Chemphyschem.*
745 18(19): 2756-2765.

746 Santhosh, C., Velmurugan, V., Jacob, G., Jeong, S.K., Grace, A.N., Bhatnagar, A., 2016. Role of
747 nanomaterials in water treatment applications: A review. *Chem. Eng. J.* 306: 1116-1137.

748 Sas, S., Danko, M., Bizovská, V., Lang, K., Bujdák, J., 2017. Highly luminescent hybrid materials
749 based on smectites with polyethylene glycol modified with rhodamine fluorophore. *Appl.*
750 *Clay. Sci.* 138: 25-33.

751 Shaikh, S.M.R., Nasser, M.S., Hussein, I., Benamor, A., Onaizi, S.A., Qiblawey, H., 2017a.
752 Influence of polyelectrolytes and other polymer complexes on the flocculation and
753 rheological behaviors of clay minerals: A comprehensive review. *Sep. Purif. Technol.* 187:
754 137-161.

755 Shaikh, S.M.R., Nasser, M.S., Hussein, I.A., Benamor, A., 2017b. Investigation of the effect of
756 polyelectrolyte structure and type on the electrokinetics and flocculation behavior of
757 bentonite dispersions. *Chem. Eng. J.* 311: 265-276.

758 Shchipunov, Y., Ivanova, N., Silant'ev, V., 2009. Bionanocomposites formed by in situ charged
759 chitosan with clay. *Green Chem.* 11(11): 1758.

760 Shchipunov, Y.A., Sarin, S.A., Silant'ev, V.E., Postnova, I.V., 2012a. Self-organization in the
761 chitosan-clay nanoparticles system regulated through polysaccharide macromolecule
762 charging. 2. Films. *Colloid. J.* 74(5): 636-644.

763 Shchipunov, Y.A., Silant'ev, V., Postnova, I., 2012b. Self-organization in the chitosan-clay
764 nanoparticles system regulated through polysaccharide macromolecule charging. 1.
765 Hydrogels. *Colloid. J.* 74(5): 627-635.

766 Sievers, D.A., Lischeske, J.J., Biddy, M.J., Stickel, J.J., 2015. A low-cost solid-liquid separation
767 process for enzymatically hydrolyzed corn stover slurries. *Bioresour. Technol.* 187:
768 37-42.

769 Silva, J.M., Reis, R.L., Mano, J.F., 2016. Biomimetic Extracellular Environment Based on Natural
770 Origin Polyelectrolyte Multilayers. *Small*, 12(32): 4308-4342.

771 Song, J., Yamagushi, T., Silva, D.J., Hubbe, M.A., Rojas, O.J., 2010. Effect of Charge Asymmetry
772 on Adsorption and Phase Separation of Polyampholytes on Silica and Cellulose Surfaces.
773 *Journal of Physical Chemistry B.* 114(2): 719-727.

774 Sposito, G., Skipper, N.T., Sutton, R., Park, S.-h., Soper, A.K., Greathouse, J.A., 1999. Surface
775 geochemistry of the clay minerals. *Proceedings of the National Academy of Sciences.*
776 96(7): 3358-3364.

777 Stöter, M., Rosenfeldt, S., Breu, J., 2015. Tunable Exfoliation of Synthetic Clays. *Annu. Rev.*
778 *Mater. Res.* 45(1): 129-151.

779 Takeno, H., Kimura, Y., 2016. Molecularweight effects on tensile properties of blend hydrogels
780 composed of clay and polymers. *Polym.* 85: 47-54.

781 Takeno, H., Nakamura, A., 2019. Effects of molecular mass of polymer on mechanical properties
782 of clay/poly (ethylene oxide) blend hydrogels, and comparison between them and
783 clay/sodium polyacrylate blend hydrogels. *Colloid. Polym. Sci.* 297(4): 641-649.

784 Takeno, H., Nakamura, W., 2013. Structural and mechanical properties of composite hydrogels
785 composed of clay and a polyelectrolyte prepared by mixing. *Colloid. Polym. Sci.* 291(6):
786 1393-1399.

787 Tarasova, E., Naumenko, E., Rozhina, E., Akhatova, F., Fakhrullin, R., 2019. Cytocompatibility
788 and uptake of polycations-modified halloysite clay nanotubes. *Appl. Clay. Sci.* 169:
789 21-30.

790 Tong, Z., Deng, Y., 2013. The formation of asymmetric polystyrene/saponite composite
791 nanoparticles via miniemulsion polymerization. *J. Appl. Polym. Sci.* 127(5): 3916-3922.

792 Van Haver, L., Nayar, S., 2017. Polyelectrolyte flocculants in harvesting microalgal biomass for
793 food and feed applications. *Algal. Res.* 24: 167-180.

794 Vereb, G., Nagy, L., Kertesz, S., Kovacs, I., Hodur, C., Laszlo, Z., 2017. Highly Efficient
795 Purification of Finely Dispersed Oil Contaminated Waters By Coagulation/Flocculation
796 Method and Effects on Membrane Filtration. *Stud. U. Babes-Bol. Che.* 62(2): 259-270.

797 Vipulanandan, C., Mohammed, A.S., 2014. Hyperbolic rheological model with shear stress limit
798 for acrylamide polymer modified bentonite drilling muds. *J. Petrol. Sci. Eng.* 122: 38-47.

799 Viseras, C., Cerezo, P., Sanchez, R., Salcedo, I., Aguzzi, C., 2010. Current challenges in clay
800 minerals for drug delivery. *Appl. Clay. Sci.* 48(3): 291-295.

801 Wang, S., Konduri, M.K.R., Hou, Q., Fatehi, P., 2016. Cationic xylan–METAC copolymer as a
802 flocculant for clay suspensions. *RSC Adv.* 6(46): 40258-40269.

803 Wang, X., Yang, L., Zhang, J., Wang, C., Li, Q., 2014. Preparation and characterization of
804 chitosan–poly (vinyl alcohol)/bentonite nanocomposites for adsorption of Hg (II) ions.
805 *Chem. Eng. J.* 251: 404-412.

806 Wang, Z., Huang, W.X., Yang, G.H., Liu, Y., Liu, S., 2019. Preparation of cellulose-base
807 amphoteric flocculant and its application in the treatment of wastewater. *Carbohydr.*
808 *Polyme*, 215: 179-188.

809 Xiao, S., Castro, R., Maciel, D., Goncalves, M., Shi, X., Rodrigues, J., Tomas, H., 2016. Fine
810 tuning of the pH-sensitivity of laponite-doxorubicin nanohybrids by polyelectrolyte
811 multilayer coating. *Mater Sci Eng C Mater Biol Appl*, 60: 348-356.

812 Yu, L., Zhang, J., Li, G., Zhao, H., Liu, T., 2018. Research and Application of Plugging Drilling
813 Fluid with Low-Activity and High Inhibition Properties. *Petroleum Drilling Techniques*,
814 46(1): 44-48.

815 Zhang, B., Su, H., Gu, X., Huang, X., Wang, H., 2013a. Effect of structure and charge of
816 polysaccharide flocculants on their flocculation performance for bentonite suspensions.
817 *Colloid. Surface. A.* 436: 443-449.

818 Zhang, J., Chen, M., Tian, J., Li, W., Xiao, J., 2005. Effect of Mixed Anionic-Cationic
819 Polyacrylamide on Rheological Properties of Smectite Gel. *Acta Petrolei Sinica*
820 *Petroleum Processing Section.* 21(3): 84.

821 Zhang, J., Wang, Q. Jiang, J., 2013b. Lime mud from paper-making process addition to food waste
822 synergistically enhances hydrogen fermentation performance. *Int. J. Hydrogen. Energy.*
823 38(6): 2738-2745.

824 Zhao, Y., Cavallaro, G., Lvov, Y., 2015. Orientation of charged clay nanotubes in evaporating
825 droplet meniscus. *J Colloid Interface Sci*, 440: 68-77.

826 Zhen, R., Chi, Q., Wang, X., Yang, K., Jiang, Y., Li, F., Xue, B., 2016. Crystallinity, ion
827 conductivity, and thermal and mechanical properties of poly (ethylene oxide)–illite
828 nanocomposites with exfoliated illite as a filler. *J. Appl. Polym. Sci.*133(47).

829 Zhou, C.H., Cun Jun, L., Gates, W.P., Zhu, T.T. and Wei Hua, Y., 2019a. Co-intercalation of
830 organic cations/amide molecules into montmorillonite with tunable hydrophobicity and
831 swellability. *Appl. Clay Sci.*179:1-11.

832 Zhou, C.H., Zhou, Q., Wu, Q.Q., Petit, S., Jiang, X.C., Xia, S.T., Li, C.S., Yu, W.H., 2019b.
833 Modification, hybridization and applications of saponite: An overview. *Appl. Clay. Sci.*
834 168: 136-154.

835 Zhou, D.J., Zhang, Z.P., Tang, J.L., Wang, F.W., Liao, L.B., 2016. Applied properties of oil-based
836 drilling fluids with montmorillonites modified by cationic and anionic surfactants. *Appl.*
837 *Clay Sci.* 121: 1-8.

838 Zhu, T.T., Zhou, C.H., Kabwe, F.B., Wu, Q.Q., Li, C.S., Zhang, J.R., 2019. Exfoliation of
839 montmorillonite and related properties of clay/polymer nanocomposites. *Appl. Clay. Sci.*
840 169: 48-66.

841